Available online at www.sciencedirect.com
ScienceDirect
Developmental Biology 315 (2008) 72–88
DEVELOPMENTAL BIOLOGY
www.elsevier.com/developmentalbiology

Attenuation of retinal vascular development and neovascularization in PECAM-1-deficient mice

Terri A. DiMaio [a], Shoujian Wang [a], Qiong Huang [a], Elizabeth A. Scheef [a], Christine M. Sorenson [b], Nader Sheibani [a,c,*]

[a] Department of Ophthalmology and Visual Sciences, University of Wisconsin School of Medicine and Public Health, Madison, WI 53792-4673, USA
[b] Department of Pediatrics, University of Wisconsin School of Medicine and Public Health, Madison, WI 53792-4673, USA
[c] Department of Pharmacology, University of Wisconsin School of Medicine and Public Health, Madison, WI 53792-4673, USA

Received for publication 22 August 2006; revised 20 November 2007; accepted 4 December 2007
Available online 22 January 2008

Abstract

Platelet–endothelial cell adhesion molecule-1 (PECAM-1/CD31) is expressed on the surface of endothelial cells (EC) at high levels with important roles in angiogenesis and inflammation. However, the physiological role PECAM-1 plays during vascular development and angiogenesis remains largely unknown. Here we determined the role of PECAM-1 in the postnatal development of retinal vasculature and retinal neovascularization during oxygen-induced ischemic retinopathy (OIR) using PECAM-1-deficient (PECAM-1−/−) mice. A significant decrease in retinal vascular density was observed in PECAM-1−/− mice compared with PECAM-1+/+ mice. This was attributed to a decreased number of EC in the retinas of PECAM-1−/− mice. An increase in the rate of apoptosis was observed in retinal vessels of PECAM-1−/− mice, which was compensated, in part, by an increase in the rate of proliferation. However, the development and regression of hyaloid vasculature were not affected in the absence of PECAM-1. We did not observe a significant defect in astrocytes, the number of endothelial tip cell filopodias, and the rate of developing retinal vasculature progression in PECAM-1−/− mice. However, we observed aberrant organization of arterioles and venules, decreased secondary branching, and dilated vessels in retinal vasculature of PECAM-1−/− mice. In addition, retinal neovascularization was attenuated in PECAM-1−/− mice during OIR despite an expression of VEGF similar to that of PECAM-1+/+ mice. Mechanistically, these changes were associated with an increase in EphB4 and ephrin B2, and a decrease in eNOS, expression in retinal vasculature of PECAM-1−/− mice. These results suggest that PECAM-1 expression and its potential interactions with EphB4/ephrin B2 and eNOS are important for survival, migration, and functional organization of EC during retinal vascular development and angiogenesis.

Keywords: CD31; Angiogenesis; Apoptosis; Retinal vascularization; Retinopathy of prematurity; Hyaloid vasculature; Retinal endothelial cells

Introduction

PECAM-1 is a member of the immunoglobulin gene superfamily of cell adhesion molecules. It is highly expressed on the surface of EC and at lower levels on the surface of platelets and hematopoietic cells. PECAM-1 is important in endothelial cell–cell interactions during monolayer formation in culture (Albelda et al., 1990) and capillary morphogenesis in Matrigel (Sheibani et al., 1997). Antibodies to PECAM-1 block angiogenesis in mouse corneal pocket assays (DeLisser et al., 1997). Furthermore, the important role of PECAM-1 in angiogenesis has been recently demonstrated in PECAM-1-deficient (PECAM-1−/−) mice. These mice exhibited defects in their angiogenesis and inflammatory responses to foreign body challenges (Graesser et al., 2002; Solowiej et al., 2003). However, the physiological role PECAM-1 plays during vascular development and angiogenesis requires further investigation.

The developing mouse retinal vasculature provides a unique opportunity to study all aspects of vascular development postnatally and is readily amenable to biochemical evaluations. Mice are born without any retinal blood vessels, which develop immediately after birth. During the first week of life, a superficial layer of vessels is formed, which sprouts perpendicularly

* Corresponding author. Department of Ophthalmology and Visual Sciences, University of Wisconsin School of Medicine and Public Health, 600 Highland Avenue, K6/458 CSC, Madison, WI 53792-4673, USA. Fax: +1 608 265 6021.
E-mail address: nsheibanikar@wisc.edu (N. Sheibani).

0012-1606/$ - see front matter © 2007 Elsevier Inc. All rights reserved.
doi:10.1016/j.ydbio.2007.12.008

deep into the retina forming the deep retinal vascular plexuses by the third week of postnatal life. Retinal vasculature continues to undergo pruning and remodeling during the next 3 weeks, and a complete vasculature is established by 6 weeks of age (Dorrell et al., 2002; Fruttiger, 2002; Michaelson et al., 1954; Wang et al., 2003).

An inherent characteristic of the developing retinal vasculature is its sensitivity to changes in oxygen levels. This is responsible for ischemia-driven retinal neovascularization, which occurs in children that are born prematurely and are exposed to high levels of oxygen in order to help with their breathing and lung development. The exposure to high oxygen results in decreased levels of proangiogenic factors promoting the loss of existing retinal blood vessels and preventing the growth of additional blood vessels. Therefore, as a result of this the retina becomes ischemic upon exposure to normal air inducing the expression of proangiogenic factors, such as VEGF. This promotes growth of new blood vessels. Unfortunately, these vessels are abnormal in function and are leaky. They grow into the vitreous where they hemorrhage resulting in retinal detachment and loss of vision. Thus, understanding the molecular and cellular mechanisms that impact retinal neovascularization will aid in the development of new strategies to intervene and prevent loss of vision.

Oxygen-induced ischemic retinopathy (OIR) in the mouse is a highly reproducible model of angiogenesis *in vivo* and recapitulates the human condition described above (Smith et al., 1994). In this model, postnatal day 7 (P7) mice are exposed to 75% oxygen for 5 days and then brought to room air for 5 days, during which time maximum retinal neovascularization occurs. To gain further insight into the physiological role PECAM-1 plays during vascular development and neovascularization, we compared the normal postnatal development of retinal vasculature and retinal neovascularization during OIR in PECAM-1+/+ and PECAM-1−/− mice. Here we demonstrate that PECAM-1−/− mice exhibit decreased retinal vascular density. This was mainly attributed to the enhanced rate of apoptosis and the decreased number of EC observed in retinal vasculature of the PECAM-1−/− mice. The retinal blood vessels were also dilated and had fewer secondary branches in these mice, perhaps through deregulated expression and/or activity of EphB4/ephrin B2 and eNOS. However, the development of the ocular embryonic (hyaloid) vessels and their regression, an apoptosis-dependent process, was not affected in PECAM-1−/− mice. Furthermore, retinal neovascularization was impaired in PECAM-1−/− mice during OIR. This was associated with the failure of PECAM-1−/− mice to up-regulate eNOS expression. These studies demonstrate an important role for PECAM-1 during normal development and remodeling of retinal vasculature and its neovascularization during OIR.

Materials and methods

Tissue preparation

The targeting of the *PECAM-1* gene and the generation of mutant mice in a C57BL/6 background were previously described (Duncan et al., 1999). PECAM-1−/− mice and wild-type mice were maintained at the University of Wisconsin animal facility and studies were performed according to approved protocols. Mice were bred for different experimental time points. For oxygen-induced ischemic retinopathy, 7-day-old (P7) pups and their mother were placed in an airtight incubator and exposed to an atmosphere of 75±0.5% oxygen for 5 days. Incubator temperature was maintained at 23±2 °C, and oxygen was continuously monitored with a PROOX model 110 oxygen controller (Reming Bioinstruments Co., Redfield, NY). Mice were brought to room air for 5 days, and then pups were sacrificed for retinal whole-mount preparations and neovascularization analysis as described below.

Trypsin-digested retinal vessel preparations

Eyes were enucleated from P21 or P42 mice and fixed in 4% paraformaldehyde for at least 24 h. The eyes were bisected equatorially and the entire retina was removed under the dissecting microscope. Retinas were washed overnight in distilled water and incubated in 3% trypsin (Trypsin 1:250, Difco) prepared in 0.1 M Tris, 0.1 M maleic acid, pH7.8 containing 0.2 M NaF for approximately 1–1.5 h at 37 °C. Following completion of digestion, retinal vessels were flattened by four radial cuts and mounted on glass slides for periodic acid-schiff (PAS) and hematoxylin staining. Nuclear morphology was used to distinguish pericytes from EC. The nuclei of EC are oval or elongated and lie within the vessel wall along the axis of the capillary, while pericyte nuclei are small, spherical, stain densely and generally have a protuberant position on the capillary wall. The stained and intact retinal whole mounts were coded, and subsequent counting was performed masked.

The numbers of EC and pericytes were determined by counting respective nuclei under the microscope at a magnification of ×400. A mounting reticle (10 μm×10 μm) was placed in one of the viewing oculars to facilitate counting. Only retinal capillaries were included in the cell count, which was performed in the mid-zone of the retina. We counted the number of EC and pericytes in four reticles from the four quadrants of each retina. The total number of EC and pericytes for each retina was determined by adding the numbers from the four reticles. The ratio of EC to pericytes was then calculated. To evaluate the density of cells in the capillaries, the mean number of EC or pericytes was recorded in four reticles from each of the four quadrants of each retina.

Visualization of retinal vasculature and quantification of the rate of vascular expansion and avascular areas during OIR

The retinal vascular pattern and vessel obliteration were analyzed using retinal whole mounts stained with anti-collagen IV antibody as described previously (Wang et al., 2003). At various times mouse eyes were enucleated and briefly fixed in 4% paraformaldehyde (10 min on ice). The eyeballs were fixed in 70% ethanol for at least 24 h at −20 °C. Retinas were dissected in PBS and then washed with PBS three times, 10 min each. Following incubation in blocking buffer (50% fetal calf serum, 20% normal goat serum in PBS) for 2 h, the retinas were incubated with rabbit anti-mouse collagen IV (Chemicon, diluted 1:500 in PBS containing 20% fetal calf serum, 20% normal goat serum) at 4 °C overnight. Retinas were then washed three times with PBS, 10 min each, incubated with secondary antibody Alexa 594 goat–anti-rabbit (molecular probes; 1:500 dilution prepared in PBS containing 20% FCS, 20% NGS) for 2 h at RT, washed four times with PBS, 30 min each, and mounted on a slide with PBS/glycerol (2 vol/1vol). Retinas were viewed by fluorescence microscopy, and images were captured in digital format using a Zeiss microscope (Carl Zeiss, Chester, VA). The relative rate of retinal vascular expansion was determined by measuring the radius of expanding retinal blood vessels relative to the radius of the retina from the optic nerve head in P5 PECAM-1+/+ and PECAM-1−/− mice. The central capillary dropout area during OIR was quantified as percentage of whole retina area. The quantitative assessments were made from the digital images in masked fashion using Axiovision software (Carl Zeiss, Chester, VA).

Quantification of neovascular proliferative retinopathy

Quantification of vitreous neovascularization on P17 was performed as previously described (Wang et al., 2003). Briefly, mouse eyes were enucleated, fixed in formalin for 24 h, and embedded in paraffin. Serial sections (6 μm

thick), each separated by at least 40 μm, were taken from around the region of the optic nerve. The hematoxylin- and PAS-stained sections were examined in masked fashion for the presence of neovascular tufts projecting into the vitreous from the retina. The neovascular score was defined as the mean number of neovascular nuclei per section found in eight sections (four on each side of the optic nerve) per eye.

BrdU and collagen IV staining of whole-mount retinas

The detection of cell proliferation on the retinal blood vessels was assessed by immunohistochemistry for 5-bromo-2-deoxyuridine (BrdU) incorporation and type IV collagen (staining blood vessels). Mice were injected intraperitoneally with 5-bromo-2-deoxyuridine (BrdU; Sigma, St. Louis, MO) 0.12 g/kg of body mass dissolved in water. One and a half hours later the animals were sacrificed, their eyes were removed, and fixed immediately in 4% paraformaldehyde for 3 min on ice. Eyes were then transferred to 70% ethanol (v/v) and stored at −20 °C for at least 2 h. Retinas were dissected in PBS, washed for 30 min in PBS containing 1% Triton X-100 to permeabilize cell membranes, and placed in 2 M HCl at 37 °C for 1 h. Each retina was then washed in 0.1 M sodium borate for 30 min to neutralize the HCl. Retinas were then washed in PBS containing 1% Triton X-100 for 15 min and incubated with a monoclonal antibody to BrdU (Cat No. 1170376, Roche, Indianapolis, IN; diluted 1:250 in PBS containing 1% bovine serum albumin, BSA) at 4 °C overnight or room temperature for 2 h. Following incubation, retinas were washed for 10 min in PBS containing 1% Triton X-100 and incubated with anti-mouse CY2 antibody (Jackson's Laboratory) diluted 1:500 in PBS containing 1% BSA for 2 h. Retinas were then washed in PBS and stained with anti-collagen IV (Chemicon) antibody as described above. The collagen IV and secondary antibodies were used at 1:1000 and 1:500, respectively. After a final wash in PBS for 30 min, the retinas were mounted with the ganglion cell layer uppermost in PBS:glycerol (2:1 v/v). Retinas were viewed by fluorescence microscopy and images were captured in digital format using a Zeiss microscope (Carl Zeiss, Chester, VA). Results are expressed as the mean number of positive staining cells per retina from five eyes of five mice. Whole-mount retinas were also stained with a rat–anti-mouse endoglin (BD Phaminogen; stain blood vessels), anti-NG2 (Chemicon; stain pericytes), rabbit–anti-GFAP (Dako; stain astrocytes), rat anti-mouse EphB4 and goat anti-mouse ephrin B2 (R&D; stain blood vessels) as recommended by the supplier.

TdT-dUTP terminal nick-end labeling of retinal vasculature

Apoptotic cell death on the retinal vasculature was assessed by TdT-dUTP terminal nick-end labeling (TUNEL) staining on trypsin-digested retinal vessels. The eyes were removed, fixed in 10% neutral formalin at 4 °C for 48 h, the eyes were bisected equatorially, and the entire retina was removed under the dissecting microscope. Retinas were washed in distilled water for 1 h and incubated in 3% trypsin (Trypsin 1:250, Difco) prepared in 0.1 M Tris, 0.1 M maleic acid, pH 7.8 containing 0.2 M NaF for approximately 40 min at 37 °C. Following completion of digestion, retinal vessels were flattened by four radial cuts, placed on a poly-L-lysine-coated glass slide, and allowed to dry. The retinal vessels were then washed in PBS for 20 min, rehydrated with PBS containing 0.5% Triton X-100 for 1 h, and washed in PBS for 20 min. The TUNEL staining was performed with the Fluorescein *in situ* Cell Death Detection kit as recommended by the supplier (Roche Indianapolis, IN). The retinal vessels were then washed with PBS for 30 min and were counterstained with Hoechst 33258 (Molecular probes, Eugene, OR) for nuclei staining for 15 min. The retinal vessels were washed in PBS for 20 min and mounted with a coverslip. Retinal vessels were viewed by fluorescence microscopy and images were captured in digital format using a Zeiss microscope (Carl Zeiss, Chester, VA). The retinas were examined using a 20× objective under the fluorescence microscope, and the number of TUNEL-positive cells in retinal vasculature was determined for each retina. Results are expressed as the mean number of positive staining cells from five eyes from five mice.

Immunohistochemical staining of the frozen sections

Mouse eyes were enucleated and embedded in optimal cutting temperature (OCT) compound at −80 °C. Sections (9 μm) were cut on a cryostat, placed on glass slides, and allowed to dry for 2 h. For fluorescence microscopy, sections were fixed in cold acetone (4 °C) on ice for 10 min, followed by three washes with PBS, 5 min each. Sections were incubated in blocker (1% BSA, 0.2% skim milk, and 0.3% Triton X-100 in PBS) for 15 min at room temperature. Sections were then incubated with rabbit anti-mouse type IV collagen antibody (Chemicon) or anti-eNOS (Santa Cruz) (1:500 dilution prepared in blocking solution) overnight at 4 °C in a humid environment. After three washes in PBS, 5 min each, sections were incubated with secondary antibody Alexa 594 goat–anti-rabbit (Molecular probes) (1:500 dilution prepared in blocking solution). Sections were washed three times in PBS, covered with PBS:glycerol (2 vol/1vol), and mounted with a coverslip. Retina sections were viewed by fluorescence microscopy, and images were captured in digital format using a Zeiss microscope (Carl Zeiss, Chester, VA).

Staining of the hyaloid vasculature

Following the removal of eyes, the sclera, choroids, and retina were dissected anteriorly from the optic nerve to limbus. The remaining whole-mount specimen was stained with FITC-conjugated B4-lectin (1:100 dilution; Sigma, St. Louis, MO) to visualize the hyaloid vasculature. Whole-mount specimens were viewed by fluorescence microscopy and images were captured in digital format using a Zeiss microscope (Carl Zeiss, Chester, VA). The dissection resulted, in most cases, in the loss of hyaloid artery and vasa hyaloidea propria vessels. However, the tunica vasculosa lentis vessels were clearly visible following lectin staining.

Western blot analysis

VEGF protein levels were determined by Western blotting of whole-eye extracts prepared from P15 mice during OIR (5 days of hyperoxia and 3 days of normoxia) when maximum levels of VEGF are expressed (Pierce et al., 1995; Wang et al., 2003). Mice were sacrificed by CO_2 inhalation, eyes were dissected, homogenized in RIPA buffer (10 mM HEPES pH 7.6, 142.5 mM KCl, 1% NP-40, and protease inhibitor cocktail; Roche Biochemicals), sonicated briefly, and incubated at 4 °C for 20 min. Homogenates were centrifuged at 16,000×*g* for 10 min at 4 °C to remove insoluble material. Clear supernatants were transferred to a clean tube and protein concentrations were determined using DC protein assay (Bio-Rad). Approximately 20 μg of protein lysates was analyzed by SDS-PAGE (4–20% Tris–glycin gel, Invitrogen, Carlsbad, CA) under reducing conditions and transferred to a Nitrocellulose membrane. For evaluation of EphB4 and ephrin B2 protein levels, retina extracts were similarly prepared from P7 mice for Western blot analysis. Blots were incubated with rabbit anti-mouse VEGF (1:2000; PeproTech, Rock hill, NJ), goat anti-mouse EphB4, or goat anti-mouse ephrin B2 (1:1000; Sigma) antibodies, washed, and developed using an appropriate HRP-conjugated secondary antibody (1:5000; Jackson Immunoresearch Laboratories, West Grove, PA) and ECL system (Amersham). The same blots were also probed with a monoclonal antibody to β-catenin (1:3000; BD transduction) or β-actin (1:5,000; Sigma) to verify equal protein loading in all lanes.

Statistical analysis

Statistical differences between groups were evaluated with Student's unpaired *t*-test (two-tailed). Mean ± standard deviation is shown. P values of <0.05 are considered significant.

Results

PECAM-1−/− mice exhibit decreased retinal vascular density

The murine retinal vasculature develops postnatally. A superficial layer of vessels is formed during the first week of postnatal life (P7). These vessels sprout and penetrate the deep retina during the second and third week of postnatal life forming the deep retinal vascular plexuses by P21 (Dorrell et al., 2002;

Fruttiger, 2002). We first compared retinal vascular densities by trypsin-digested preparation of retinas from P21 (when primary vascularization of retina is complete) and P42 (when remodeling and pruning of vasculature are complete) mice. Fig. 1 shows a representative retinal trypsin digest prepared from P42 PECAM-1+/+ (A) and PECAM-1−/− (B) mice. We observed a significant decrease in cellularity and capillary loops in retinas from PECAM-1−/− mice compared to wild-type mice. Table 1 shows the endothelial cell-to-pericyte ratios (*E*/*P*) in retinal trypsin digests prepared from PECAM-1+/+ and PECAM-1−/− mice. There were no significant differences in the *E*/*P* ratios of PECAM-1+/+ and PECAM-1−/− mice ($P>0.05$) at P21 and P42. These mice exhibited an *E*/*P* of (3:1) at P21 and (2:1) at P42, as was shown previously for the wild-type mice (Wang et al., 2003). The association of pericytes with retinal vasculature was also confirmed by immunofluorescence staining of whole-mount retinal vasculature using antibodies to endoglin (stain EC) and NG2 (stain pericytes) (not shown). Thus, the decrease in retinal vascular density of PECAM-1−/− mice is associated with a decrease in the number of EC and pericytes.

We next determined the densities of EC and pericytes in the retinal trypsin digests. Table 2 and Table 3 show the density of EC and pericytes, respectively. The densities of EC and pericytes were significantly lower in PECAM-1−/− mice at P21 and P42 compared to PECAM-1+/+ mice ($P<0.05$). In addition, the retinal vessels in PECAM-1−/− mice had a larger diameter compared with PECAM-1+/+ mice, which was quantitatively assessed in whole-mount collagen IV staining of retinal vasculature (see below). The appearance of the basement membrane of these vessels was less smooth and somewhat thicker than retinal vessels in PECAM-1+/+ mice (Figs. 1B and 2H). Together, these studies indicated that the PECAM-1−/− retinal vasculature was at lower density and abnormal in appearance.

The course of retinal vessel sprouting and assembly can be readily visualized by collagen IV staining of whole-mount retinal preparations. We next evaluated the retinal vasculature of PECAM-1−/− mice at different postnatal days of development by collagen IV staining of whole-mount preparations. Figs. 2A and B show the developing retinal vessels in P7 PECAM-1+/+ and PECAM-1−/− mice, respectively. The decrease in retinal vascular density is readily detectable at this stage (Figs. 2C and D). The arteriole and venule distribution was clearly visible between major veins and arteries of the PECAM-1+/+ mice, but it became less dense and their distinction was less apparent in PECAM-1−/− mice. There was also a significant decrease in secondary branching of the retinal vessels off the main radial blood vessels in PECAM-1−/− mice (Figs. 2E and F). The mean number of secondary branches off the major vessels per length in wild-type mice was 8±2 while in PECAM-1−/− mice, it was 4±1 ($P<0.05$). The diameters of blood vessels were larger in PECAM-1−/− mice compared to wild-type mice (Figs. 2E and F; 13±2 μm vs. 6±1 μm; $P<0.05$). The heterogeneity in the size of blood vessels was also visible in frozen sections prepared from P21 PECAM-1−/− mice compared with PECAM-1+/+ mice (Figs. 2G and H). These sections were stained with an antibody to fibronectin which localizes to the basement membrane of retinal blood vessels. The retinal vessels in PECAM-1−/− mice appeared dilated and contained increased amounts of fibronectin in their basement membrane. This is consistent with the abnormal appearances of vessels observed in the trypsin digest preparations of PECAM-1−/− mice (Fig. 1).

To determine whether the changes observed in retinal vasculature of PECAM-1−/− is related to alterations in guidance, endothelial tip cells and stalk behavior, or expansion velocity of the EC, we examined retinal vasculature from P5 mice. At this stage the superficial layer of retinal vessels has not reached the periphery, thus, allowing the evaluation of retinal vessels progression and interactions with astrocytes. Normally, astrocytes have already reached the periphery ahead of the developing vasculature at this stage. Antibodies to GFAP and endoglin

Table 1
E/*P* ratios in wild-type and PECAM-1−/− mice divided according to age (mean±SD)

Age, days	Wild type	PECAM-1−/−
21	3.09±0.13 (8)	3.13±0.19 (8)[a]
42	2.33±0.17 (8)	2.26±0.32 (8)[a]

[a] $P>0.05$. The number of retinas (mice) counted is given in parentheses.

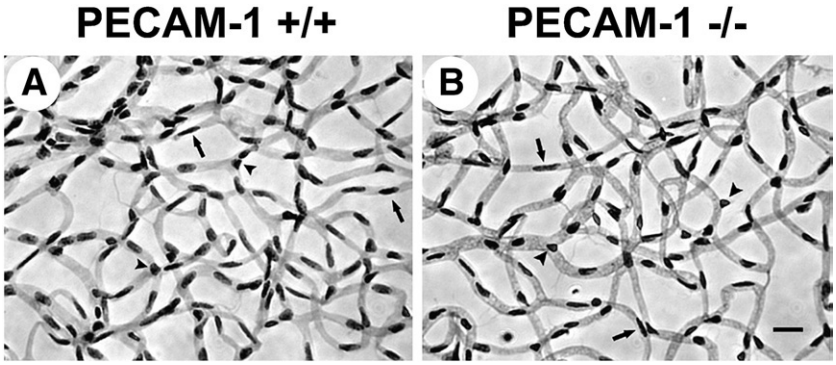

Fig. 1. Mouse retinal vasculature prepared by trypsin digestion technique. Retinas were obtained from P42 wild-type (A) or PECAM-1−/− mice (B). The arrows indicate EC, while arrowheads show the pericytes lining the retinal capillaries. Please note the decreased number of capillary loops as well as abnormal appearance of capillaries in the PECAM-1−/− retina. The quantitative assessment of the data is shown in Tables 1–3. Scale bar=20 μm (A and B).

Table 2
Number of EC per reticle square (100 μm^2) in wild-type and PECAM-1−/− mice divided according to age (density, mean±SD)

Age, days	Wild type	PECAM-1−/−
21	142.4±9.0 (6)	92.3±6.3 (8)[a]
42	118.0±7.2 (8)	68.4±4.8 (8)[a]

[a] $P<0.01$. The number of retinas (mice) counted is given in parentheses.

were used to visualize the developing retinal vasculature and its association with the scaffolding laid down by the astrocytes. The GFAP staining indicated that the astrocytes have similarly migrated to the retinal periphery in PECAM-1+/+ and PECAM-1−/− mice laying a scaffolding that is normally followed by EC (Figs. 3A and B). Endoglin staining showed similar organization of tip cells and stalk behavior in expanding retinal vasculature with and without PECAM-1 (Figs. 3C and D). Figs. 3E and F show that PECAM-1+/+ and PECAM-1−/− EC similarly following the scaffolding laid down by astrocytes. Furthermore, the mean number of tip cell filopodias per retina of PECAM-1−/− mice was not significantly different from that of PECAM-1+/+ mice (Fig. 3G; $P>0.05$). We observed no significant difference in the rate of retinal blood vessel expansion between PECAM-1+/+ and PECAM-1−/− mice (not shown). Thus, lack of PECAM-1 minimally affected the spreading of astrocytes to the retina periphery and their coverage by retinal EC through similar organization of endothelial tip cells and coverage by pericytes.

Our collagen IV staining of retinal whole mounts indicated abnormal organization and reduced density of arterioles and venules between major arteries and veins in PECAM-1−/− mice (Fig. 2). Ephrins and their receptors (Ephs) play an important role in vascular patterning and homeostasis (Erber et al., 2006). The postnatal developing mouse retinal vasculature expresses ephrin B2 which is exclusive to the arteries (Claxton and Fruttiger, 2005). However, the expression of EphB4 was not exclusive to veins and was expressed in other vessels at lower levels. Our preliminary gene expression analysis of PECAM-1+/+ and PECAM-1−/− brain EC indicated increased expression of EphB4 and ephrin B2 in null cells. We next examined whether the expression of EphB4 and ephrin B2 is altered in retinal vasculature of PECAM-1−/− mice. The staining of PECAM-1+/+ and PECAM-1−/− retinal whole mounts with endoglin showed the decreased retinal vascular density and aberrant organization of arterioles and venules in PECAM-1−/− mice (Figs. 4A and B; see the area marked with an oval). We also observed a significant EphB4 staining in retinal vasculature of PECAM-1−/− mice compared to PECAM-1+/+ mice, which was not restricted to the veins (Figs. 4C and D). However, despite several attempts and antibodies from several sources we were unable to detect ephrin B2 in retinal whole-mount staining. We next examined the levels of EphB4 and ephrin B2 in retina extracts prepared from wild-type and PECAM-1−/− mice by Western blot analysis. We observed increased levels of EphB4 and ephrin B2 in retinas of PECAM-1−/− mice (Fig. 4E). Thus, lack of PECAM-1 was associated with increased levels of EphB4 and ephrin B2.

Enhanced rates of apoptosis and proliferation in retinal vasculature of PECAM-1−/− mice

PECAM-1 is important for EC survival (Bird et al., 1999; Evans et al., 2000; Ferrero et al., 2003; Gao et al., 2003; Limaye et al., 2005). We next determined the rate of apoptosis in the retinal vasculature of PECAM-1+/+ and PECAM-1−/− mice by TUNEL staining of whole-mount retinal trypsin digests. This allowed identification of the apoptotic cells as vascular cells that are associated with the retinal blood vessels. Fig. 5 shows a significant increase in the rates of apoptosis observed in the retinal vasculature of 2- and 3-week-old PECAM-1−/− mice (Figs. 5B and F) compared to PECAM-1+/+ mice (Figs. 5A and E). The quantitative comparisons are shown in Fig. 5I ($P<0.05$).

To determine whether increased apoptosis in PECAM-1−/− mouse retinal vasculature was compensated for, in part, by an increase in cell proliferation, BrdU labeling was used. Fig. 6 shows a significant increase in the number of cells proliferating in the retinal vasculature of PECAM-1−/− mice compared with PECAM-1+/+ mice (Figs. 6A, C and B, D). The quantitative assessment of the data is shown in Fig. 6E ($P<0.01$). Thus, the lack of PECAM-1 in the retinal vascular EC impairs their survival, which may contribute to the reduced retinal vascular density.

The development and regression of hyaloid vasculature were not affected in the PECAM-1−/− mice

We next asked whether lack of PECAM-1 affects the development and regression of ocular embryonic (hyaloid) vessels. The papillary membrane and hyaloid vessels (hyaloid arteries, tunica vasculosa lentis, and vasa hyaloidea propria) provide nourishment to the immature lens, retina, and vitreous (Ito and Yoshioka, 1999). However, they regress by apoptosis during the later stages of ocular development. We evaluated the status of hyaloid vasculature by B4-Lectin staining of ocular specimens prepared from PECAM-1+/+ and PECAM-1−/− mice. Fig. 7 shows the staining of the hyaloid vasculature (mainly tunica vasculosa lentis) in whole-mount ocular specimens prepared from PECAM-1+/+ and PECAM-1−/− mice at 1 week (A and B), 2 weeks (C and D), and 3 weeks (E and F) of age. We observed a significant number of hyaloid vessels in wild-type and PECAM-1−/− mice by 1 week of age (Figs. 7A and B). However, these vessels regressed similarly in the wild-type and PECAM-1−/− mice by 3 weeks of age (Figs. 7E and F), and by 6 weeks of age complete regression of the hyaloid vessels was noted (not shown). Therefore, absence of PECAM-1 does not impact the development and/or regression of hyaloid vessels.

Table 3
Number of pericytes per reticle square (100 μm^2) in wild-type and PECAM-1−/− mice divided according to age (density, mean±SD)

Age, days	Wild type	PECAM-1−/−
21	68.4±2.9 (8)	44.7±2.6 (8)[a]
42	53.0±4.2 (8)	37.6±2.7 (8)[b]

[a] $P<0.01$. The number of retinas (mice) counted is given in parentheses.
[b] $P<0.05$.

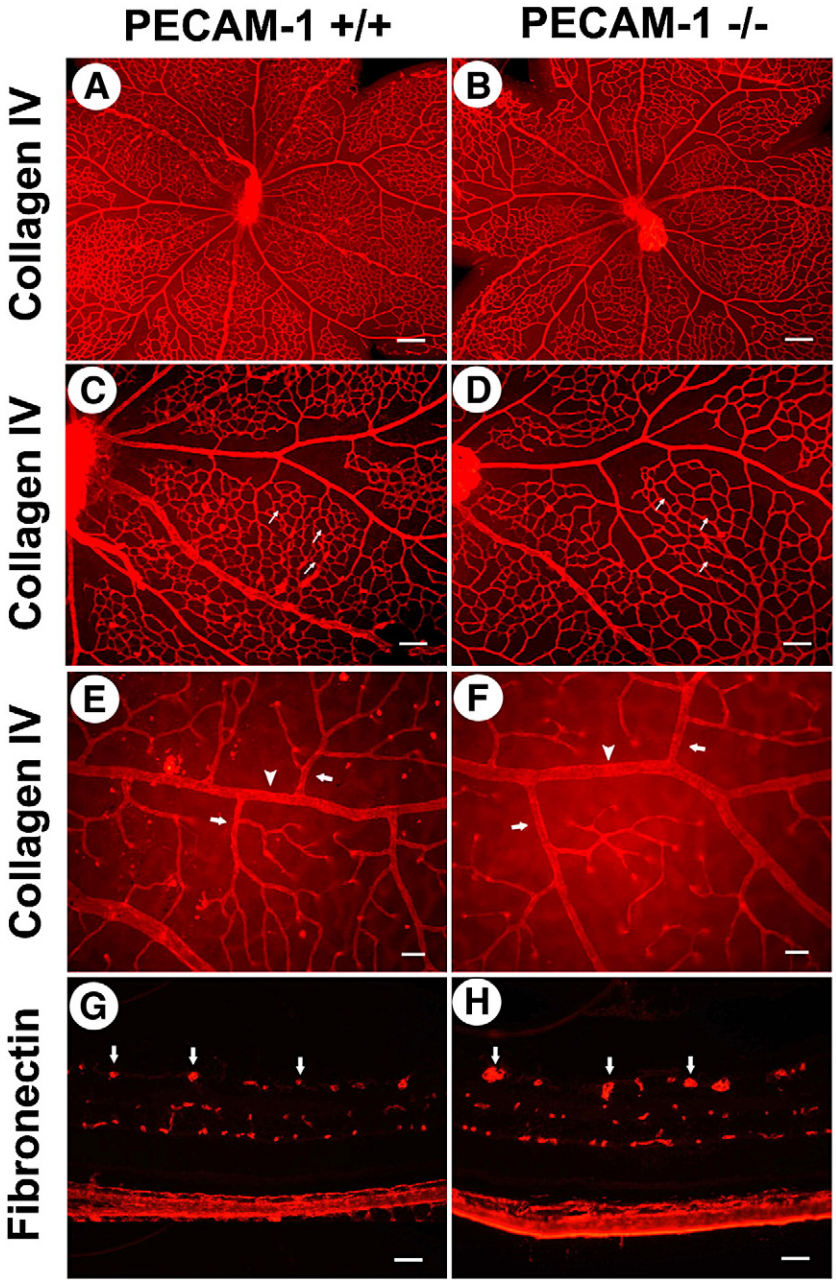

Fig. 2. Collagen IV staining of the retinal whole mounts prepared from PECAM-1+/+ and PECAM-1−/− mice. Retinas were obtained from 1 (A–D)- or 6-week-old (E–F) wild-type (A, C, E) and PECAM-1−/− (B, D, F) mice and stained with an anti-collagen IV antibody as described in Materials and methods. Arrows indicate decreased number of capillary loops in retinas from PECAM-1−/− (D) compared with retinas from PECAM-1+/+ (C) mice. Please note decreased number of secondary branches off major arteries in retinas from PECAM-1−/− (F) compared with retinas from PECAM-1+/+ (E, arrows) mice. Arrowheads in panels E and F point to a major artery. Please note the larger diameter of arteries in retinas of PECAM-1−/− mice. Panels G and H show fibronectin staining of frozen sections prepared from PECAM-1+/+ (G) and PECAM-1−/− (H) mice. Please note increased fibronectin staining in the retinal vessels of PECAM-1−/− mice which are dilated compared to PECAM-1+/+ mice (arrows). These experiments were repeated three times with similar results. Scale bars: A and B = 200 μm; C and D = 100 μm; E and F = 20 μm; G and H = 50 μm.

The developing retinal vasculature of PECAM-1−/− mice showed similar sensitivity to hyperoxia-mediated vessel obliteration as PECAM-1+/+ mice during OIR

The oxygen-induced ischemic retinopathy (OIR) in the mouse is a highly reproducible model for studying all aspects of angiogenesis. In this model, P7 mice are exposed to 75% oxygen for 5 days and then returned to room air for 5 days. The exposure of the developing retinal vasculature to high oxygen prevents the growth of additional vessels and promotes loss of existing vessels due to diminished expression of VEGF (Smith et al., 1994; Wang et al., 2003). Therefore, when animals are returned to room air, the retina becomes ischemic and promotes the growth of new blood vessels, which grow into the vitreous and bleed.

We next compared the response of PECAM-1−/− and PECAM-1+/+ mice to OIR. Figs. 8A and B show whole-

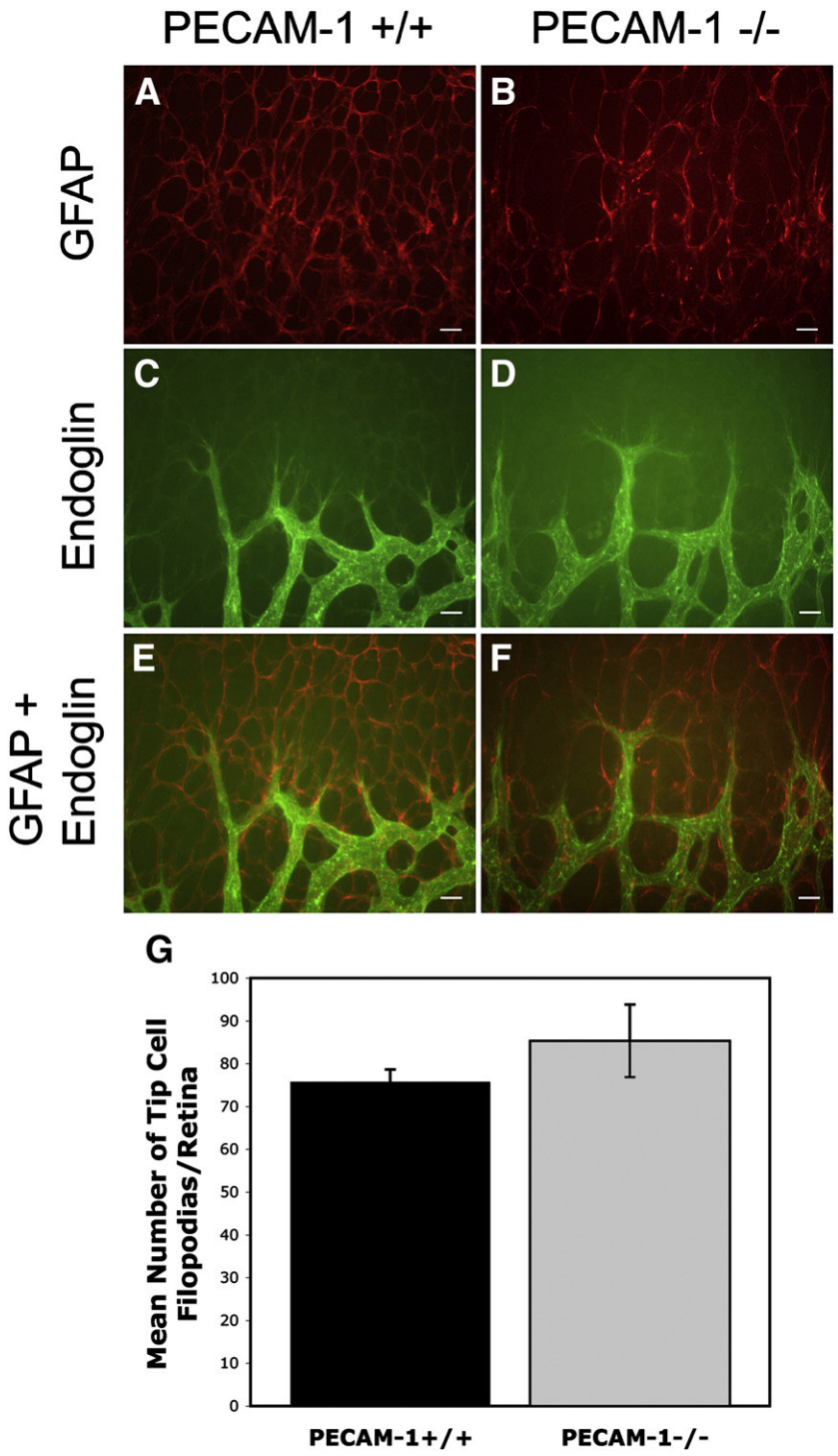

Fig. 3. Astrocytic organization, formation of tip cells, and retinal vasculature expansion are not affected in the absence of PECAM-1. Whole-mount retinas from PECAM-1+/+ (A, C, and E) and PECAM-1−/− (B, D, and F) P5 mice were stained with antibodies to GFAP (A and B) or endoglin (C and D). The merged images are shown in panels E and F. The quantitative assessment of tip cell's filopodia is shown in panel G. Data in each bar are the mean number of filopodias counted in five retinas from five different mice. Please note similar organization and expansion of astrocytic template in PECAM-1+/+ and PECAM-1−/−. The endothelial tip cells similarly followed the astrocytic template without a significant difference in the number of tip cell filopodias. Other experiments were repeated twice with eyes from four different mice. Scale bar=20 μm.

mount collagen IV staining of the retinal vasculature in P12 mice during OIR. The exposure of these mice to 5 days of hyperoxia (P12) resulted in the obliteration of blood vessels in the central area of the retina. The quantitative assessment of nonperfused areas of retina from PECAM-1+/+ and PECAM-1−/− mice is shown in Fig. 8C. We observed a similar degree of vessel obliteration in wild-type and PECAM-1−/− mice. Thus, lack of PECAM-1 does not significantly impact hyperoxia-mediated vessel obliteration during OIR.

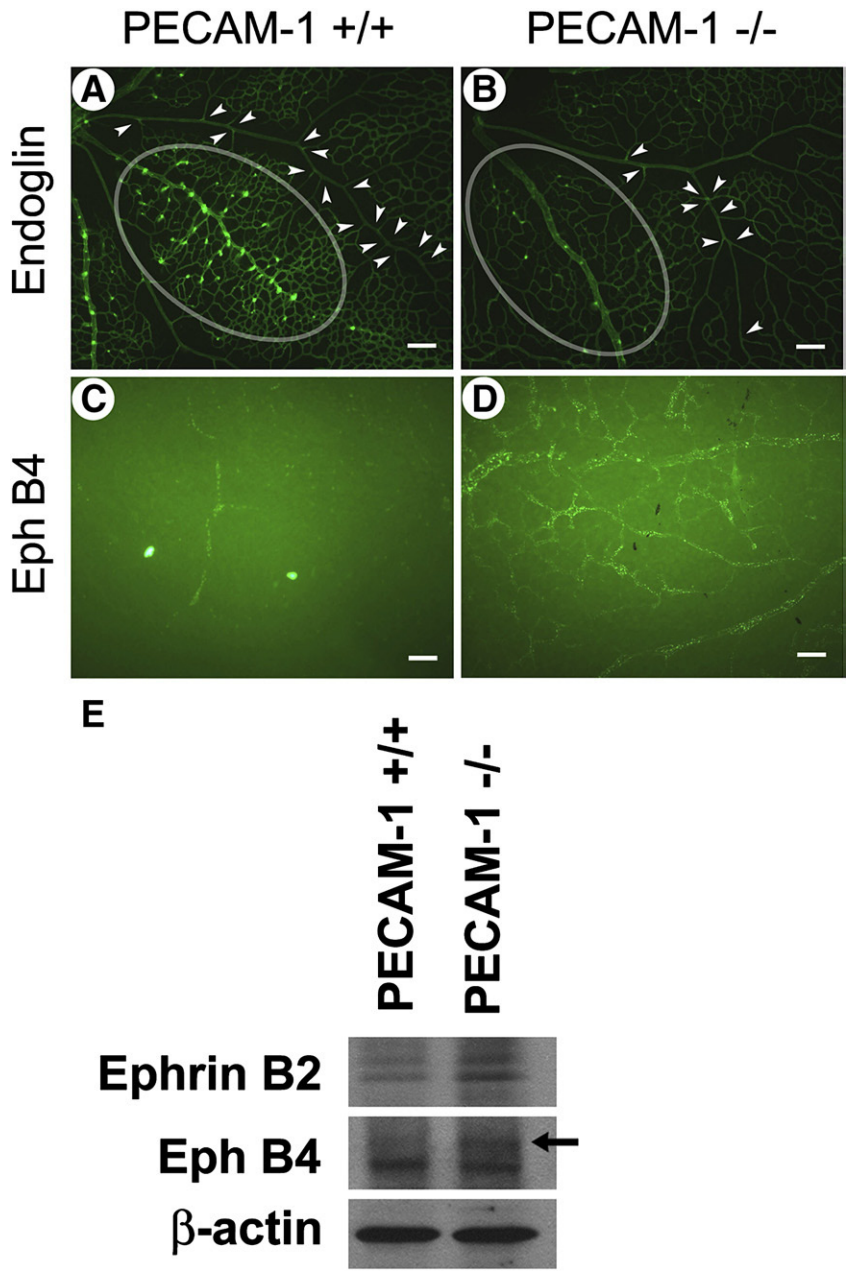

Fig. 4. Aberrant organization of arterioles and venules and expression of EphB4 and ephrin B2 in retinal vasculature of PECAM-1−/− mice. Whole-mount retinas from P7 PECAM-1+/+ (A and C) and PECAM-1−/− (B and D) mice were stained with endoglin (A and B) or EphB4 (C and D). The exposure times were identical. The ovals in panels A and B mark an area where arterioles and venules are organizing. Please note the reduced density and aberrant organization of the arterioles and venules, and decreased secondary branching (arrowheads) in PECAM-1−/− mice. In addition, retinal vasculature of PECAM-1−/− mice showed significantly increased staining for EphB4. We were unable to detect ephrin B2 in retinal whole mounts using antibodies from multiple sources. Panel E shows a Western blot of retinal extracts prepared from P7 PECAM-1+/+ and PECAM-1−/− mice and probed for EphB4 and ephrin B2 as described in Materials and methods. The blot was also probed with anti-β-actin to control for loading. These experiments were repeated three times with eyes from three different mice. Scale bar = 50 μm.

The exposure of the P12 mice to room air (5 days) results in an ischemic retina and aggressive growth of new blood vessels by P17. Neovascularization occurs in the retinal periphery, and sprouting of new vessels from the existing larger vessels in the nonperfused area is observed which is dependent on the expression of VEGF. Figs. 9A and B show whole-mount collagen IV staining of the retinal vasculature in P17 mice subjected to OIR. In PECAM-1+/+ mice, a robust neovascular response was observed as expected. In contrast, the neovascular response during OIR was significantly attenuated in PECAM-1−/− mice. Thus, expression of PECAM-1 is essential for the growth of new vessels.

Quantification of preretinal neovascularization

Quantification of preretinal neovascularization on P17 mice (when maximum neovascularization occurs) was performed as previously described by us (Wang et al., 2003). Briefly, 6-μm-

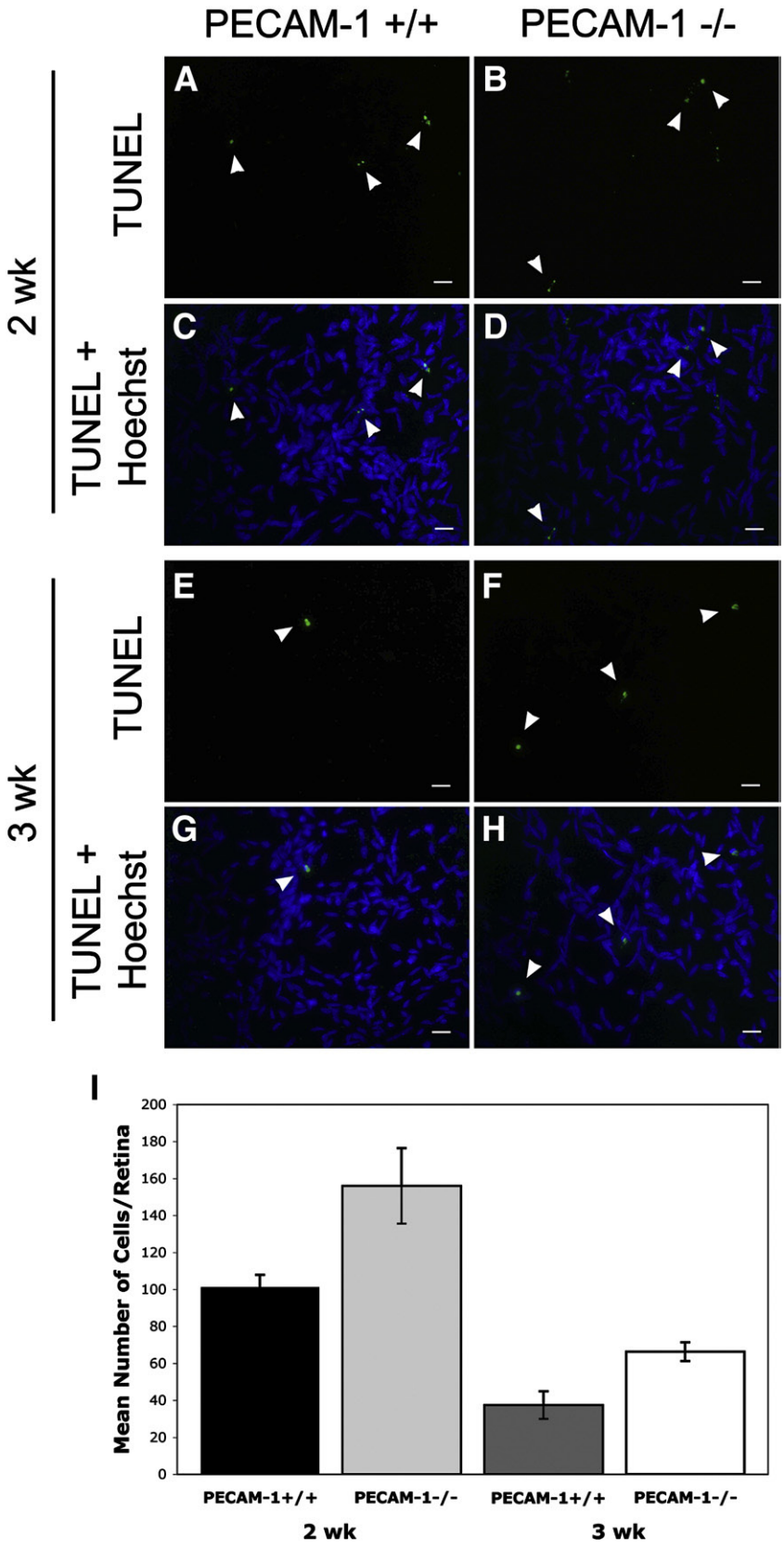

Fig. 5. Increased rates of apoptosis in retinal vasculature of PECAM-1−/− mice. Whole-mount trypsin-digested retinal vasculature were prepared from 2 (A–D)- or 3-week (E–H)-old PECAM-1+/+ and PECAM-1−/− mice and processed for TUNEL staining as described in Materials and methods. Panels A, B, E, and F show TUNEL staining (arrowheads). Panels C, D, G, and H show the merged TUNEL and Hoechst staining. The quantitative analysis of the data is shown in panel I. Data in each bar are the mean number of TUNEL-positive cells per retina in five eyes of five mice (error bar indicate standard deviation). Please note a significant increase in the rate of apoptosis in PECAM-1−/− retinas compared to wild-type mice ($P<0.01$). These experiments were repeated twice with similar results. Scale bar=100 μm.

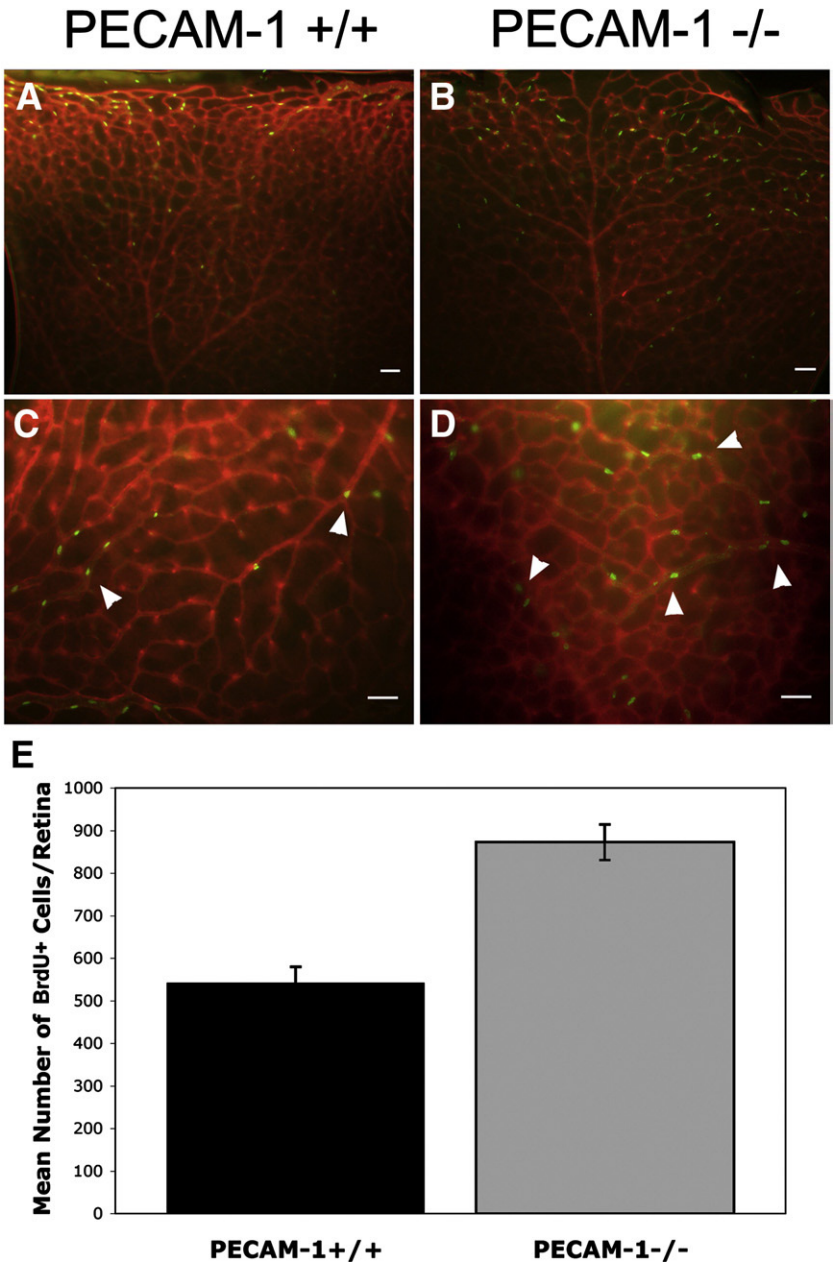

Fig. 6. Enhanced cell proliferation in retinal vasculature of PECAM-1−/− mice. Proliferating cells in P14 PECAM-1+/+ (A and C) and PECAM-1−/− (B and D) mice were labeled by BrdU and detected using an antibody to BrdU as described in Materials and methods. Collagen IV staining was used to visualize the vasculature. Quantitative assessment of cell proliferation on the retinal vessels is shown in panel D. Data in each bar are the mean number of $BrdU^+$ cells per retina of five eyes of five mice (error bar indicate standard deviation). Please note that the number of proliferating cells is significantly higher in PECAM-1−/− retina compared to wild-type ($P<0.01$). Scale bars: A and B = 100 μm; C and D = 50 μm.

thick serial sections, each separated by at least 40 μm, were obtained from the region around the optic nerve. The sections were stained with hematoxylin and PAS and examined in masked fashion for the presence of neovascular cell nuclei projecting into the vitreous from the retina (Figs. 9C and D). The neovascular cell nuclei score was defined as the mean number of neovascular nuclei per section found in eight sections (four on each side of the optic nerve) per eye. Fig. 9E shows the mean number of vascular cell nuclei projecting into the vitreous of eyes from wild-type and PECAM-1−/− mice. There were significantly less vascular cell nuclei detected in the P17 PECAM-1−/− mice compared to the PECAM-1+/+mice ($P<0.05$). This is mainly attributed to the lack of PECAM-1, which is essential for survival of vascular cells during angiogenesis. Therefore, expression of PECAM-1 contributes to neovascularization of the retina in response to ischemia.

Lack of PECAM-1 did not affect VEGF expression during OIR

To determine whether the inability of retinas from PECAM-1−/− mice to undergo neovascularization in response to ischemia was due to lack of VEGF expression, we examined

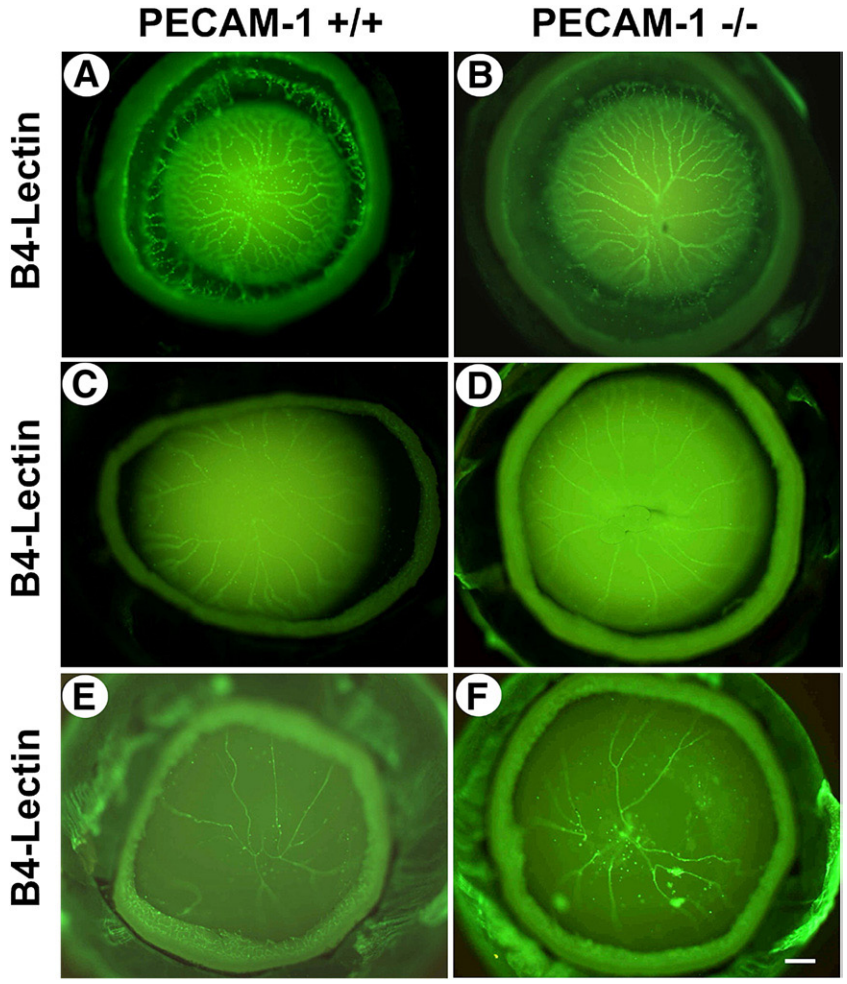

Fig. 7. Assessment of hyaloid vasculature in wild-type and PECAM-1−/− mice. The whole-mount staining of hyaloid vasculature from wild-type (A, C, and E) and PECAM-1−/− (B, D, and F) mice at 1 week (A and B), 2 weeks (C and D), and 3 weeks (E and F) of age were prepared as described in Materials and methods. Please note similar vascularization and regression of vasculature in wild-type and PECAM-1−/− mice at all time points. Scale bar=200 μm.

VEGF levels in eyes from P15 wild-type and PECAM-1−/− mice (5 days of hyperoxia and 3 days of normoxia). VEGF expression is maximally induced during OIR at P15 (Pierce et al., 1995; Wang et al., 2003). Fig. 10 shows a Western blot of total protein lysates prepared from whole eye extracts of PECAM-1+/+ and PECAM-1−/− P15 mice during OIR. We observed similar levels of VEGF expression in eyes from P15 wild-type and PECAM-1−/− mice during OIR. Therefore, the lack of retinal neovascularization in the absence of PECAM-1 is not due to insufficient amounts of VEGF expression.

Decreased levels of endothelial nitric oxide synthase (eNOS) in PECAM-1−/− mice

The predominant NOS expressed in EC is eNOS, and it catalyzes the formation of NO from L-arginine, which results in the activation of soluble guanylyl cyclase and initiation of various signaling cascades with important roles in vascular homeostasis (Forstermann and Munzel, 2006). The eNOS is recently shown to associate with PECAM-1 and localizes to cell–cell junctions, and this association results in inhibition of eNOS activity (Dusserre et al., 2004a; Govers et al., 2002). However, phosphorylation of PECAM-1 upon shear stress leads to dissociation of eNOS from PECAM-1, thus activating eNOS (Bagi et al., 2005b). To determine whether expression of eNOS is affected in the absence of PECAM-1, we stained histological sections from P15 PECAM-1+/+ and PECAM-1−/− mice reared in normal air or during OIR with antibody to eNOS (Fig. 11). We observed a significant decrease in eNOS staining of retinal blood vessels of PECAM-1−/− mice compared with PECAM-1+/+ mice reared in normal air (Figs. 11A and B, arrows). In P15 mice during OIR (5 days of hyperoxia and 3 days of room air), we observed a significant up-regulation of eNOS expression in PECAM-1+/+ mice (Fig. 11C). This is consistent with active retinal neovascularization and proangiogenic activity of eNOS in PECAM-1+/+ mice. In sharp contrast, no significant level of eNOS was detected in retinal vasculature of PECAM-1−/− mice during OIR (Fig. 11D), which also failed to undergo active neovascularization (Fig. 9). These observations are consistent with vasodilatory defects reported in PECAM-1−/− mice arterioles and lack of eNOS junctional localization in PECAM-1−/− EC (Bagi et al., 2005b). Furthermore, the eNOS−/− mice, like PECAM-1−/− mice, show significant reduction in retinal neovascularization during OIR

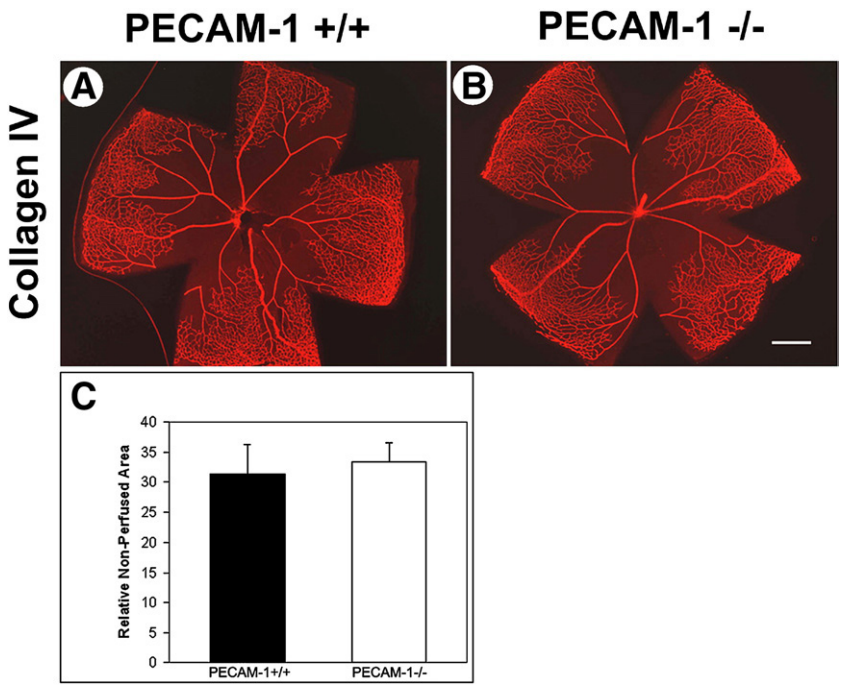

Fig. 8. Quantitative assessments of the retinal nonperfused areas in response to hyperoxia. Whole-mount retinas prepared from P12 wild-type (A) or PECAM-1−/− (B) mice exposed to 5 days of hyperoxia were stained with antibody to collagen IV. Relative nonperfused areas of retinas were determined as described in Materials and methods (C). Data in each bar are the mean nonperfused area relative to whole area of each retina in five eyes of five mice (error bars indicate standard deviation). Please note that there is no significance difference in the degree of vessel obliteration in response to hyperoxia in wild-type and PECAM-1−/− mice ($P=0.73$). Scale bar=500 μm.

(Brooks et al., 2001; Yu et al., 2005). Thus, the lack of PECAM-1 may contribute to dysregulation of eNOS expression and/or activity and decreased neovascularization.

Discussion

PECAM-1/CD31 is an EC adhesion molecule capable of initiating outside-in and inside-out signals which impact cell adhesive and migratory properties (Kondo et al., 2007; Wang and Sheibani, 2006). Although PECAM-1 has been implicated in endothelial cell–cell interactions during angiogenesis, little is known about its physiological function during vascular development and angiogenesis. Here we show that PECAM-1 expression is important for normal development of the retinal vasculature and neovascularization during OIR. PECAM-1−/− mice exhibited reduced vascular density, abnormal branching morphogenesis, and blood vessels with a larger diameter. The decreased vascular density was attributed, at least in part, to increased rates of apoptosis in retinal vasculature of PECAM-1−/− mice. This was somewhat compensated by an increase in the rate of cell proliferation in PECAM-1−/− mice. Lack of PECAM-1 had minimal effects on the development and regression of hyaloid vasculature. Given the fact that PECAM-1 can directly interact with eNOS and ephrin B2, it is reasonable to speculate that changes in the expression and/or activity of these genes may occur in the absence of PECAM-1. We observed increased levels of EphB4 and its ligand ephrin B2 and decreased levels of eNOS in retinal vasculature of PECAM-1−/− mice. Thus, PECAM-1 may play an important role in EC survival, migration, and functional organization during vascular development and angiogenesis through modulation of eNOS and EphB4/ephrin B2 expression and/or activity.

PECAM-1 and postnatal retinal vascularization

Retinal vascular development in the mouse occurs postnatally. Our trypsin-digested whole-mount retinal preparations (Fig. 1) and quantitative evaluation of EC and pericyte ratios and densities (Tables 1–3) indicated a significant decrease in the density of retinal vessels in PECAM-1−/− mice. This was further confirmed by whole-mount staining of the retinal vasculature at different postnatal times (Figs. 2 and 4). There is a significant decrease in cellularity and capillary loops in retinas of P7 PECAM-1−/− mice ((Figs. 1, 2C, D and 4A)). We did not observe a significant difference in endothelial tip cell filopodias and stalk behavior, retinal vessels expansion velocity, or astrocytic guidance of retinal EC in PECAM-1−/− mice compared to PECAM-1+/+ mice (Fig. 3). However, the organization of arterioles and venules between major arteries and veins appeared abnormal and less dense in PECAM-1−/− mice compared to PECAM-1+/+ mice. A significant decrease in secondary branching of the blood vessels, which occurs off the major vessels, was also observed in PECAM-1−/− mice.

EphB4 and its preferred ligand ephrin B2 signaling play an important role in blood vessel morphogenesis and patterning, as well as blood vessel permeability (Claxton and Fruttiger, 2005; Oike et al., 2002). Capillary plexuses remodeling is defective in EphB4 or ephrin-B2-deficient mice leading to early embryonic

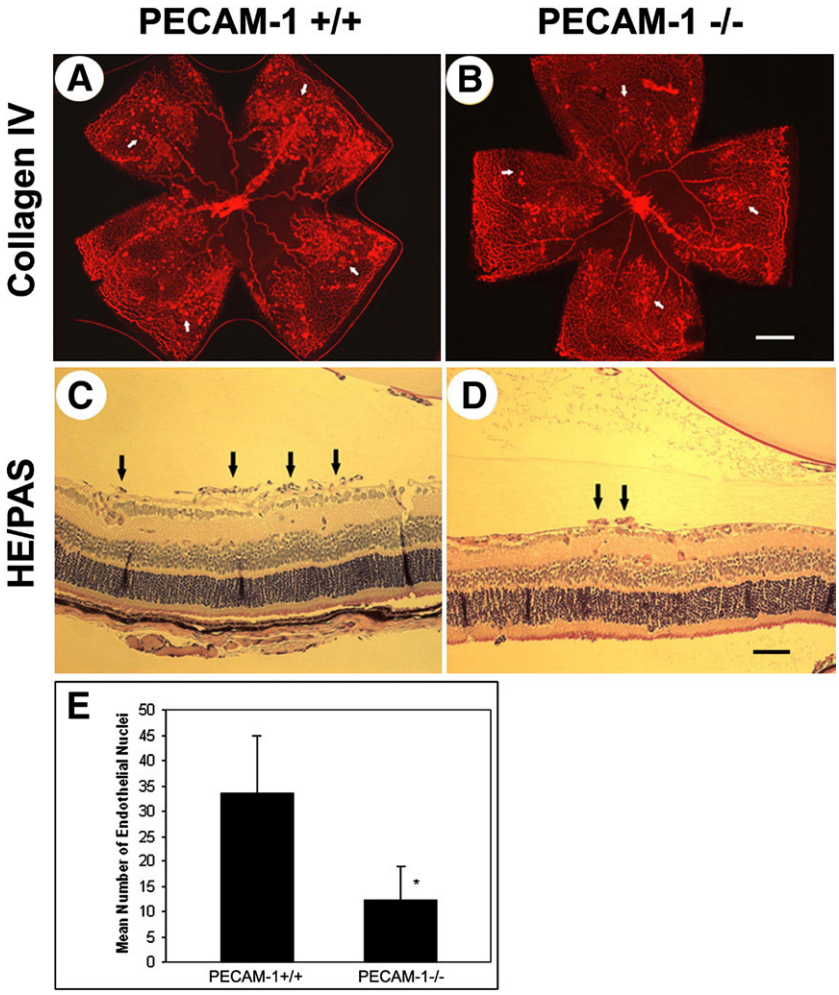

Fig. 9. Quantitative assessment of neovascularization in P17 mice exposed to a cycle of hyperoxia and room air (OIR). Panels A and B are collagen IV stained whole-mount retinas, while panels C and D are HE/PAS-stained eye sections prepared from P17 wild-type and PECAM-1−/− mice, respectively. The arrows indicate growth of new vascular tufts which are significantly diminished in PECAM-1−/− mice. The number of vascular cell nuclei present on the vitreous side of the retina penetrating the inner limiting membrane was determined as described in Materials and methods (E). Data in each bar are the mean number of vascular cell nuclei in five eyes of five mice (error bars indicate standard deviation). Please note that there is a significant decrease in the degree of retinal neovascularization in PECAM-1−/− mice compared with wild-type mice ($P<0.01$). Scale bars: A and B = 500 μm; C and D = 50 μm.

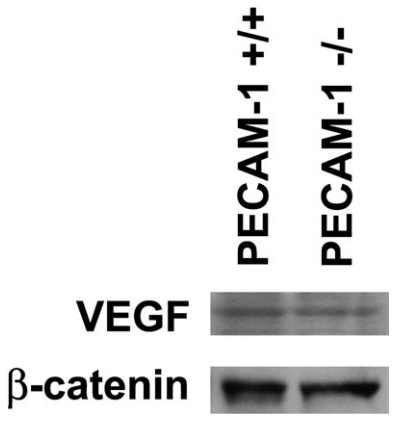

Fig. 10. Assessment of VEGF levels in eyes from PECAM-1+/+ and PECAM-1−/− mice. Eye extracts prepared from PECAM-1+/+ and PECAM-1−/− P15 mice (5 days of hyperoxia and 3 days of normoxia) were analyzed by SDS-PAGE and Western blotting as described in Materials and methods. β-Catenin was used as a loading control. These experiments were repeated twice with eyes from three different mice with similar results.

lethality (Gerety et al., 1999; Wang et al., 1998). Recent studies also indicate that ephrin B2 and/or EphB4 are not just intrinsic EC differentiation markers and their expression is controlled by microenvironmental determinants, including hypoxia, VEGF, shear stress and contact with smooth muscle cells (Claxton and Fruttiger, 2005; Fruttiger, 2007; Goettsch et al., 2004; Korff et al., 2006; Taylor et al., 2007). The developing mouse retinal vasculature expresses EphB4 and ephrin B2 mRNA (Claxton and Fruttiger, 2005). In addition, cultured retinal and choroidal EC express EphB4 and ephrin B2 and their signaling impacts cell proliferation and migration (Kim et al., 2002; Saint-Geniez et al., 2003; Steinle et al., 2002, 2003). Furthermore, soluble forms of EphB4 and ephrin B2 are shown to inhibit retinal and choroidal neovascularization *in vivo* and EC migration and capillary morphogenesis *in vitro* (He et al., 2005; Zamora et al., 2005). Thus, sustained EphB4/ephrin B2 signaling in the absence of PECAM-1 may contribute to abnormal retinal vascular development and neovascularization. However, the contribution of this signaling pathway

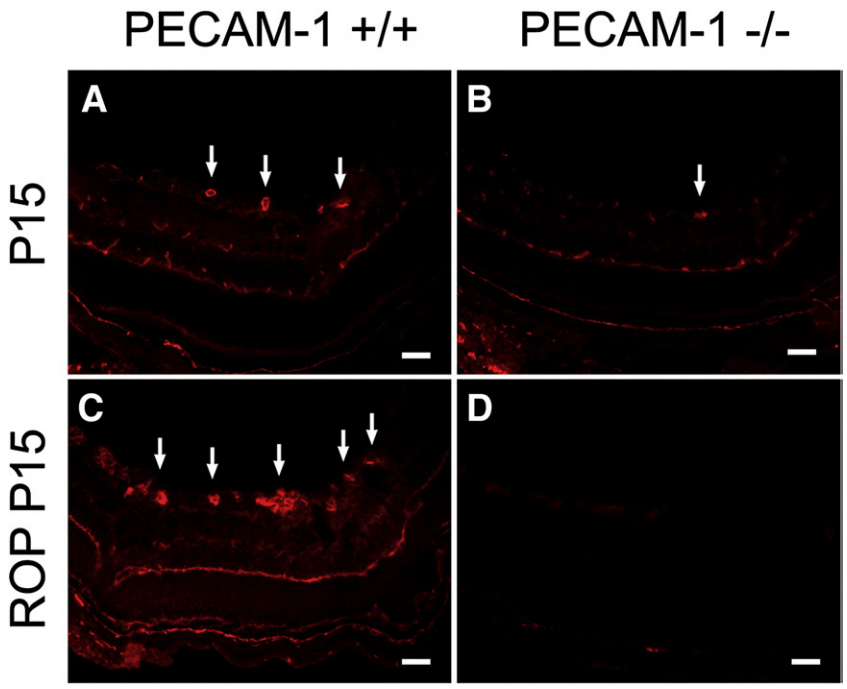

Fig. 11. Reduced expression of eNOS in retinal vasculature of PECAM-1−/− mice. Retinal frozen sections prepared from P15 PECAM-1+/+ (A and C) and PECAM-1−/− (B and D) grown in room air (A and B) or exposed to OIR (5 days of hyperoxia and 3 days of room air) (C and D) were stained with an antibody to eNOS as described in Materials and methods. All exposures were identical. Please note the PECAM-1+/+ retinal vasculature stained significantly stronger for eNOS, especially during OIR, when retinal neovascularization is occurring (arrows). These experiments were repeated three times with eyes from three different mice. Scale bar=100 μm.

to retinal vascular development and angiogenesis requires further investigation.

Our preliminary gene expression analyses indicated that the expression of EphB4 and ephrin B2 is up-regulated in PECAM-1−/− brain EC (not shown). We also observed a significant increase in EphB4 staining of vasculature (Figs. 4C, D), as well as EphB4 and ephrin B2 protein levels (Fig. 4E) in retinas of PECAM-1−/− mice. In addition, association of ephrin B2 with PECAM-1, an EphB4-dependent process, regulates its appropriate localization and function in EC (Korff et al., 2006). Thus, increased levels of EphB4/ephrin B2 and disruption of ephrin B2 association with PECAM-1 in null mice may have severe consequences on retinal vascularization. In fact, endothelial over-expression of EphB4 results in large, malformed, and cell-rich blood vessels composing an irregular vascular pattern in the retina (Erber et al., 2006). Blood vessel branching is also altered resulting in a disorganized retinal angioarchitecture. These observations are consistent with a significant decrease in secondary branching which occurs off major vessels and the presence of blood vessels with a larger diameter in PECAM-1−/− mice. Thus, sustained EphB4 and ephrin B2 signaling in PECAM-1−/− retinal vessels may act as a negative regulator of blood vessel branching and vascular network formation, and increased EC proliferation. This may further contribute to impaired interconnection of angiogenic sprouts and vascular network formation resulting in a significant reduction in branching points (Erber et al., 2006). Our results suggest that in the absence of PECAM-1, the ephrin B2/EphB4 signaling is sustained, contributing to the abnormalities observed in the PECAM-1−/− retinal vasculature. To our knowledge this is the first report of a role for PECAM-1 in arteriovenous organization, branching morphogenesis, and blood vessel diameter during vascular development. Future work is required to determine how PECAM-1 interaction with ephrin B2 impacts its interactions with EphB4 and downstream signaling events.

The decrease in retinal vascular density of PECAM-1−/− mice may also be attributed, at least in part, to an increased rate of apoptosis in the retinal vasculature of PECAM-1−/− mice. PECAM-1 was recently shown to protect EC from apoptosis in response to a number of stimuli (Bird et al., 1999; Evans et al., 2000; Ferrero et al., 2003; Gao et al., 2003; Limaye et al., 2005). The molecular mechanisms which mediate PECAM-1 survival activity in EC remain unclear and may depend on activation of MAPK/ERKs and Akt1. PECAM-1 was recently shown to be essential for activation of these signaling pathways in response to shear stress and production of nitric oxide (Fleming et al., 2005; Tai et al., 2005). Nitric oxide is a promigratory and angiogenic signal for EC. The details of how PECAM-1 activates these signaling pathways remain unknown. However, their activation is dependent on interaction of PECAM-1 cytoplasmic domain with specific intracellular signaling molecules (Wang and Sheibani, 2006). Interaction of PECAM-1 with SHP2 is important in the activation of MAPK/ERKs in response to shear stress (Tai et al., 2005). Therefore, the ability of PECAM-1 to activate MAPK/ERKs may enhance EC survival and migration during angiogenesis (Wang and Sheibani, 2006).

PECAM-1 and hyaloid vasculature

Given the important role of PECAM-1 in EC survival, we determined whether lack of PECAM-1 affects the development and regression of hyaloid vasculature. The papillary membrane and hyaloid vessels (hyaloid arteries, tunica vasculosa lentis, and vasa hyaloidea propria) provide nourishment to the immature lens, retina, and vitreous (Ito and Yoshioka, 1999). However, they regress during the later stages of ocular development. Our results indicated that the lack of PECAM-1 had minimal effect on the development and regression of these vessels.

PECAM-1 and retinal neovascularization

The developing retinal vasculature is inherently sensitive to changes in oxygen levels and its exposure to high oxygen could lead to growth of new vessels which are abnormal in function. The PECAM-1−/− mice exhibited a similar sensitivity to hyperoxia-mediated vessel obliteration compared with PECAM-1+/+ mice during OIR. Therefore, lack of PECAM-1 does not impact the sensitivity of retinal EC to hyperoxia-mediated vessel obliteration. However, PECAM-1−/− mice were impaired in their ability to neovascularize the retina during exposure to room air. This observation is consistent with the ability of antibodies to PECAM-1 to block capillary morphogenesis *in vitro* (Sheibani et al., 1997) and angiogenesis *in vivo* (DeLisser et al., 1997). Furthermore, we have shown that primary kidney EC prepared from PECAM-1−/− mice are less migratory and fail to undergo capillary morphogenesis in Matrigel (Kondo et al., 2007). The mechanisms by which lack of PECAM-1 inhibits angiogenesis are not clearly understood. Our analysis of VEGF levels during OIR indicated that lack of PECAM-1 had minimal effects on VEGF expression in retinal vasculature. However, interaction of PECAM-1 with intracellular signaling proteins can activate proangiogenic signaling pathways impacting EC adhesive and migratory properties (Kondo et al., 2007; Wang and Sheibani, 2006). Understanding how these signaling events are initiated and their impact on EC adhesion and migration would provide additional insight into the role of PECAM-1 in vascular development and neovascularization.

PECAM-1 and eNOS expression

PECAM-1 is recently shown to be essential for shear stress-induced activation of endothelial nitric oxide synthase (eNOS) and dilation of arteries in response to temporal shear stress (Bagi et al., 2005a; Tzima et al., 2005). The postnatal retinal vasculature develops normally in mice deficient in eNOS (eNOS−/−), perhaps through a compensation by neuronal NOS (Al-Shabrawey et al., 2003). However, eNOS−/− mice share some of the phenotypes observed in PECAM-1−/− mice including impaired lung function (DeLisser et al., 2006; Han and Stewart, 2006) and retinal neovascularization (Ando et al., 2002; Brooks et al., 2001 and current study). Furthermore, shear stress is a major determinant of arteriovenous differentiation, and it affects endothelial ephrin B2 expression (Goettsch et al., 2004; Le Noble et al., 2004). Therefore, eNOS may be an important target for PECAM-1-mediated vascular functions during vascular development and angiogenesis. PECAM-1 can directly associate with eNOS in EC and modulate its activity (Dusserre et al., 2004b). This interaction is very sensitive to rapid changes in fluid shear stress by adjusting the diameters of blood vessels to accommodate flow (Cheng et al., 2005). The presence of blood vessels with a larger diameter in PECAM-1−/− mice could be explained, at least in part, by reported increased levels of nitric oxide detected in coronary arteries of PECAM-1−/− mice (Liu et al., 2006). The eNOS association with PECAM-1 in EC inhibits its activity (Dusserre et al., 2004b), and its dissociation from PECAM-1 upon shear stress results in its activation (Fleming et al., 2005; Tai et al., 2005). This is consistent with increased levels of nitric oxide detected in arterioles of PECAM-1−/− mice (Liu et al., 2006). We observed a significant decrease in the amount of eNOS expressed in retinal vasculature of PECAM-1−/− mice. Furthermore, there was no induction of eNOS expression in retinal vasculature of PECAM-1−/− mice during OIR consistent with attenuation of retinal neovascularization in these mice. We also observed similar levels of Akt1 in retinal vasculature of PECAM-1+/+ and PECAM-1−/− mice (not shown). Thus, expression of PECAM-1 may be essential for appropriate expression and function of eNOS. However, the PECAM-1-dependent molecular and signaling mechanisms that modulate eNOS activity and/or expression, and the impact of eNOS activity on retinal EC adhesion, migration, and capillary morphogenesis require investigation.

In summary, PECAM-1 expression is important for EC survival, migration, and capillary morphogenesis. We show in PECAM-1−/− mice that the postnatal development of retinal vasculature and neovascularization is impaired. There is a significant decrease in vascular density due to an increased rate of apoptosis in vascular EC. Furthermore, the organization of arterioles and venules, as well as secondary branching off the major vessels, is compromised in the absence of PECAM-1. In addition, the vessels in the PECAM-1−/− mice exhibited larger diameters, perhaps due to deregulated expression and/or activity of eNOS and EphB4/ephrin-B2 signaling. The retinal neovascularization in PECAM-1−/− mice during OIR was also severely impaired. Thus, PECAM-1 plays an important role in survival, migration, and functional organization of EC during vascular development and angiogenesis and may provide an alternative target for modulation of angiogenesis.

Acknowledgments

This research was supported in part by National Institute of Health grants EY16695 (N.S.) and DK67120 (C.M.S.). N.S. is a recipient of the Career Development Award from Research to Prevent Blindness, and a Research Award from American Diabetes Association. T.A.D. is a recipient of a predoctoral fellowship from American Heart Association, 0510047Z. We thank Dr. Tak Mak (University of Toronto, Canada) for providing us with the PECAM-1−/− mice.

References

Al-Shabrawey, M., El-Remessy, A., Gu, X., Brooks, S.S., Hamed, M.S., Huang, P., Caldwell, R.B., 2003. Normal vascular development in mice deficient in endothelial NO synthase: possible role of neuronal NO synthase. Mol. Vision 9, 549–558.

Albelda, S.M., Oliver, P.D., Romer, L.H., Buck, C.A., 1990. EndoCAM: a novel endothelial cell–cell adhesion molecule. J. Cell Biol. 110, 1227–1237.

Ando, A., Yang, A., Mori, K., Yamada, H., Yamada, E., Takahashi, K., Saikia, J., Kim, M., Melia, M., Fishman, M., Huang, P., Campochiaro, P.A., 2002. Nitric oxide is proangiogenic in the retina and choroid. J. Cell. Physiol. 191, 116–124.

Bagi, Z., Frangos, J.A., Yeh, J.-C., White, C.R., Kaley, G., Koller, A., 2005a. PECAM-1 mediates NO-dependent dilation of arterioles to high temporal gradients of shear stress. Arterioscler., Thromb., Vasc. Biol. 25, 1590–1595.

Bagi, Z., Frangos, J.A., Yeh, J.C., White, C.R., Kaley, G., Koller, A., 2005b. PECAM-1 mediates NO-dependent dilation of arterioles to high temporal gradients of shear stress. Arterioscler., Thromb., Vasc. Biol. 25, 1590–1595.

Bird, I.N., Taylor, V., Newton, J.P., Spragg, J.H., Simmons, D.L., Salmon, M., Buckley, C.D., 1999. Homophilic PECAM-1(CD31) interactions prevent endothelial cell apoptosis but do not support cell spreading or migration. J. Cell Sci. 112, 1989–1997.

Brooks, S.E., Gu, X., Samuel, S., Marcus, D.M., Bartoli, M., Huang, P.L., Caldwell, R.B., 2001. Reduced severity of oxygen-induced retinopathy in eNOS-deficient mice. Invest. Ophthalmol. Visual Sci. 42, 222–228.

Cheng, C., van Haperen, R., de Waard, M., van Damme, L.C.A., Tempel, D., Hanemaaijer, L., van Cappellen, G.W.A., Bos, J., Slager, C.J., Duncker, D.J., van der Steen, A.F.W., de Crom, R., Krams, R., 2005. Shear stress affects the intracellular distribution of eNOS: direct demonstration by a novel *in vivo* technique. Blood 106, 3691–3698.

Claxton, S., Fruttiger, M., 2005. Oxygen modifies artery differentiation and network morphogenesis in the retinal vasculature. Dev. Dyn. 233, 822–828.

DeLisser, H.M., Christofidou-Solomidou, M., Strieter, R.M., Burdick, M.D., Robinson, C.S., Wexler, R.S., Kerr, J.S., Garlanda, C., Merwin, J.R., Madri, J.A., Albelda, S.M., 1997. Involvement of endothelial PECAM-1/CD31 in angiogenesis. Am. J. Pathol. 151, 671–677.

DeLisser, H.M., Helmke, B.P., Cao, G., Egan, P.M., Taichman, D., Fehrenbach, M., Zaman, A., Cui, Z., Mohan, G.S., Baldwin, H.S., Davies, P.F., Savani, R.C., 2006. Loss of PECAM-1 function impairs alveolarization. J. Biol. Chem. 281, 8724–8731.

Dorrell, M.I., Aguilar, E., Friedlander, M., 2002. Retinal vascular development is mediated by endothelial filopodia, a preexisting astrocytic template and specific R-cadherin adhesion. Invest. Ophthalmol. Visual Sci. 43, 3500–3510.

Duncan, G.S., Andrew, D.P., Takimoto, H., Kaufman, S.A., Yoshida, H., Spellberg, J., Luis de la Pompa, J., Elia, A., Wakeham, A., Karan-Tamir, B., Muller, W.A., Senaldi, G., Zukowski, M.M., Mak, T.W., 1999. Genetic evidence for functional redundancy of platelet/endothelial cell adhesion molecule-1 (PECAM-1): CD31-deficient mice reveal PECAM-1-dependent and PECAM-1-independent functions. J. Immunol. 162, 3022–3030.

Dusserre, N., L'Heureux, N., Bell, K.S., Stevens, H.Y., Yeh, J., Otte, L.A., Loufrani, L., Frangos, J.A., 2004a. PECAM-1 interacts with nitric oxide synthase in human endothelial cells: implication for flow-induced nitric oxide synthase activation. Arterioscler., Thromb., Vasc. Biol. 24, 1796–1802.

Dusserre, N., L'Heureux, N., Bell, K.S., Stevens, H.Y., Yeh, J., Otte, L.A., Loufrani, L., Frangos, J.A., 2004b. PECAM-1 interacts with nitric oxide synthase in human endothelial cells: implication for flow-induced nitric oxide synthase activation. Arterioscler., Thromb., Vasc. Biol. 24, 1796–1802.

Erber, R.E.U., Powajbo, V., Korn, T., Djonov, V., Lin, J., Hammes, H.P., Grobholz, R., Ullrich, A., Vajkoczy, P., 2006. EphB4 controls blood vascular morphogenesis during postnatal angiogenesis. EMBO J. 25, 627–641.

Evans, P.C., T.E., Kilshaw, P.J., 2000. Signaling through CD31 protects endothelial cells from apoptosis. Transplantation 71, 457–460,.

Ferrero, E., Belloni, D., Contini, P., Foglieni, C., Ferrero, M.E., Fabbri, M., Poggi, A., Zocchi, M.R., 2003. Transendothelial migration leads to protection from starvation-induced apoptosis in CD34+CD14+ circulating precursors: evidence for PECAM-1 involvement through Akt/PKB activation. Blood 101, 186–193.

Fleming, I., Fisslthaler, B., Dixit, M., Busse, R., 2005. Role of PECAM-1 in the shear-stress-induced activation of Akt and the endothelial nitric oxide synthase (eNOS) in endothelial cells. J. Cell Sci. 118, 4103–4111.

Forstermann, U., Munzel, T., 2006. Endothelial nitric oxide synthase in vascular disease: from marvel to menace. Circulation 113, 1708–1714.

Fruttiger, M., 2002. Development of the mouse retinal vasculature: angiogenesis versus vasculogenesis. Invest. Ophthalmol. Visual Sci. 43, 522–527.

Fruttiger, M., 2007. Development of the retinal vasculature. Angiogenesis 10, 77–88.

Gao, C., Sun, W., Christofidou-Solomidou, M., Sawada, M., Newman, D.K., Bergom, C., Albelda, S.M., Matsuyama, S., Newman, P.J., 2003. PECAM-1 functions as a specific and potent inhibitor of mitochondrial-dependent apoptosis. Blood 102, 169–179.

Gerety, S.S., Wang, H.U., Chen, Z.F., Anderson, D.J., 1999. Symmetrical mutant phenotypes of the receptor EphB4 and its specific transmembrane ligand ephrin-B2 in cardiovascular development. Mol. Cell 4, 403–414.

Goettsch, W., Augustin, H.G., Morawietz, H., 2004. Down-regulation of endothelial ephrinB2 expression by laminar shear stress. Endothelium 11, 259–265.

Govers, R., Bevers, L., de Bree, P., Rabelink, T.J., 2002. Endothelial nitric oxide synthase activity is linked to its presence at cell–cell contacts. Biochem. J. 361, 193–201.

Graesser, D., Solowiej, A., Bruckner, M., Osterweil, E., Juedes, A., Davis, S., Ruddle, N.H., Engelhardt, B., Madri, J.A., 2002. Altered vascular permeability and early onset of experimental autoimmune encephalomyelitis in PECAM-1-deficient mice. J. Clin. Invest. 109, 383–392.

Han, R.N.N., Stewart, D.J., 2006. Defective lung vascular development in endothelial nitric oxide synthase-deficient mice. Trends Cardiovasc. Med. 16, 29–34.

He, S., Ding, Y., Zhou, J., Krasnoperov, V., Zozulya, S., Kumar, S.R., Ryan, S.J., Gill, P.S., Hinton, D.R., 2005. Soluble EphB4 regulates choroidal endothelial cell function and inhibits laser-induced choroidal neovascularization. Invest. Ophthalmol. Visual Sci. 46, 4772–4779.

Ito, M., Yoshioka, M., 1999. Regression of the hyaloid vessels and pupillary membrane of the mouse. Anat. Embryol. 200, 403–411.

Kim, I., Ryu, Y.S., Kwak, H.J., Ahn, S.Y., Oh, J.L., Yancopoulos, G.D., Gale, N.W., Koh, G.Y., 2002. EphB ligand, ephrinB2, suppresses the VEGF- and angiopoietin 1-induced Ras/mitogen-activated protein kinase pathway in venous endothelial cells. FASEB J. 16, 1126–1128.

Kondo, S., Scheef, E.A., Sheibani, N., Sorenson, C.M., 2007. PECAM-1 isoform-specific regulation of kidney endothelial cell migration and capillary morphogenesis. Am. J. Physiol.: Cell. Physiol. 292, C2070–C2083.

Korff, T., Dandekar, G., Pfaff, D., Fuller, T., Goettsch, W., Morawietz, H., Schaffner, F., Augustin, H.G., 2006. Endothelial ephrinB2 is controlled by microenvironmental determinants and associates context-dependently with CD31. Arterioscler., Thromb., Vasc. Biol. 26, 468–474.

le Noble, F., Moyon, D., Pardanaud, L., Yuan, L., Djonov, V., Matthijsen, R., Breant, C., Fleury, V., Eichmann, A., 2004. Flow regulates arterial-venous differentiation in the chick embryo yolk sac. Development 131, 361–375.

Limaye, V., Li, X., Hahn, C., Xia, P., Berndt, M.C., Vadas, M.A., Gamble, J.R., 2005. Sphingosine kinase-1 enhances endothelial cell survival through a PECAM-1-dependent activation of PI-3K/Akt and regulation of Bcl-2 family members. Blood 105, 3169–3177.

Liu, Y., Bubolz, A.H., Shi, Y., Newman, P.J., Newman, D.K., Gutterman, D.D., 2006. Peroxynitrite reduces the endothelium-derived hyperpolarizing factor component of coronary flow-mediated dilation in PECAM-1-knockout mice. Am. J. Physiol.: Regul. Integr. Comp. Physiol. 290, R57–R65.

Michaelson, I.C., Herz, N., Lewkowitz, E., Kertesz, D., 1954. Effect of increased oxygen on the development of the retinal vessels; an experimental study. Br. J. Ophthalmol. 38, 577–587.

Oike, Y., Ito, Y., Hamada, K., Zhang, X.-Q., Miyata, K., Arai, F., Inada, T., Araki, K., Nakagata, N., Takeya, M., Kisanuki, Y.Y., Yanagisawa, M., Gale,

N.W., Suda, T., 2002. Regulation of vasculogenesis and angiogenesis by EphB/ephrin-B2 signaling between endothelial cells and surrounding mesenchymal cells. Blood 100, 1326–1333.

Pierce, E.A., Avery, R.L., Foley, E.D., Aiello, L.P., Smith, L.E.H., 1995. Vascular endothelial growth factor/vascular permeability factor expression in a mouse model of retinal neovascularization. Proc. Natl. Acad. Sci. 92, 905–909.

Saint-Geniez, M., Argence, C.B., Knibiehler, B., Audigier, Y., 2003. The *msr/apj* gene encoding the apelin receptor is an early and specific marker of the venous phenotype in the retinal vasculature. Gene Expression/Patterns 3, 467–472.

Sheibani, N., Newman, P.J., Frazier, W.A., 1997. Thrombospondin-1, a natural inhibitor of angiogenesis, regulates platelet–endothelial cell adhesion molecule-1 expression and endothelial cell morphogenesis. Mol. Biol. Cell 8, 1329–1341.

Smith, L.E., Wesolowski, E., McLellan, A., Kostyk, S.K., D'Amato, R., Sullivan, R., D'Amore, P.A., 1994. Oxygen-induced retinopathy in the mouse. Invest. Ophthalmol. Visual Sci. 35, 101–111.

Solowiej, A., Biswas, P., Graesser, D., Madri, J.A., 2003. Lack of platelet endothelial cell adhesion molecule-1 attenuates foreign body inflammation because of decreased angiogenesis. Am. J. Pathol. 162, 953–962.

Steinle, J.J., Meininger, C.J., Forough, R., Wu, G., Wu, M.H., Granger, H.J., 2002. Eph B4 receptor signaling mediates endothelial cell migration and proliferation via the phosphatidylinositol 3-kinase pathway. J. Biol. Chem. 277, 43830–43835.

Steinle, J.J., Meininger, C.J., Chowdhury, U., Wu, G., Granger, H.J., 2003. Role of ephrin B2 in human retinal endothelial cell proliferation and migration. Cell Signalling 15, 1011–1017.

Tai, L.-k., Zheng, Q., Pan, S., Jin, Z.-G., Berk, B.C., 2005. Flow activates ERK1/2 and endothelial nitric oxide synthase via a pathway involving PECAM1, SHP2, and Tie2. J. Biol. Chem. 280, 29620–29624.

Taylor, A.C., Murfee, W.L., Peirce, S.M., 2007. EphB4 expression along adult rat microvascular networks: EphB4 is more than a venous specific marker. Microcirculation 14, 253–267.

Tzima, E., Irani-Tehrani, M., Kiosses, W.B., Dejana, E., Schultz, D.A., Engelhardt, B., Cao, G., DeLisser, H., Schwartz, M.A., 2005. A mechanosensory complex that mediates the endothelial cell response to fluid shear stress. Nature 437, 426–431.

Wang, H.U., Chen, Z.F., Anderson, D.J., 1998. Molecular distinction and angiogenic interaction between embryonic arteries and veins revealed by ephrin-B2 and its receptor Eph-B4. Cell 93, 741–753.

Wang, S., Wu, Z., Sorenson, C.M., Lawler, J., Sheibani, N., 2003. Thrombospondin-1-deficient mice exhibit increased vascular density during retinal vascular development and are less sensitive to hyperoxia-mediated vessel obliteration. Dev. Dyn. 228, 630–642.

Wang, Y., Sheibani, N., 2006. PECAM-1 isoform-specific activation of MAPK/ERKs and small GTPases: implications in inflammation and angiogenesis. J. Cell. Biochem. 98, 451–468.

Yu, J., deMuinck, E.D., Zhuang, Z., Drinane, M., Kauser, K., Rubanyi, G.M., Qian, H.S., Murata, T., Escalante, B., Sessa, W.C., 2005. Endothelial nitric oxide synthase is critical for ischemic remodeling, mural cell recruitment, and blood flow reserve. Proc. Natl. Acad. Sci. 102, 10999–11004.

Zamora, D.O., Davies, M.H., Planck, S.R., Rosenbaum, J.T., Powers, M.R., 2005. Soluble forms of ephrinB2 and EphB4 reduce retinal neovascularization in a model of proliferative retinopathy. Invest. Ophthalmol. Visual Sci. 46, 2175–2182.